Laser Physics, Vol. 12, No. 2, 2002, pp. 292–299.
Original Text Copyright © 2002 by Astro, Ltd.
Copyright © 2002 by MAIK "Nauka/Interperiodica" (Russia).

Temporal Dynamics of Local Optical Responses and Sub-fs Pulse Generation in Semicontinuous Metal Films

V. A. Podolskiy[1], A. K. Sarychev[2], and V. M. Shalaev[2]

[1] *Physics Department, New Mexico State University, NM 88003-8001*

[2] *School of Electrical and Computer Engineering, Purdue University, West Lafayette, IN, 47907-1285 USA*

e-mail: vpodolsk@nmsu.edu

Received September 4, 2001

Abstract—In metal–dielectric percolation films, plasmon modes are localized in nm-sized areas, "hot-spots," where EM-field is extremely enhanced. When the excitation pulse has a broad spectrum, sub-femtosecond optical responses can occur locally on such films. Thus, sub-wavelength spatial localization and sub-light-period time localization are both possible in metal–dilectric percolation films.

1. INTRODUCTION

The optical properties of metal–dielectric films are actively studied during the past decade because of a number of novel applications they can offer in the areas of photonics, spectroscopy, and optoelectronics (see, for example, [1–4] and references therein). Metal–dielectric films close to the percolation threshold, which are also referred to as semicontinuous metal films, have particularly interesting properties that dramatically differ from the properties of both components, metal and dielectric, forming the percolation film. A key property here is spatial localization of plasmon modes, which has been theoretically predicted by Shalaev and Sarychev and experimentally verified in [3, 4]. A typical size of plasmon localization can be as small as 10 nm; the spatial distribution of the localized plasmons is highly dependent on the incident light wavelength.

This paper is concerned with the temporal behavior of the spatially localized plasmon modes. We demonstrate here that the *local* optical responses in semicontinuous metal films can experience giant field fluctuations that are far shorter than the excitation pulse duration and, in some cases, shorter than the light single cycle. This, in particular, makes possible generation of sub-fs pulses. We also show that the temporal dynamics of localized plasmons is highly dependent on the incident laser-pulse characteristics. Large and ultrashort local field fluctuations have also been predicted for other random structures, such as fractal clusters [5]. In the present paper, we demonstrate that semicontinuous metal films offer a number of advantages in generating of ultra-short pulses. Such films can simultaneously provide sub-wavelength (down to 10 nm) localization, in the space domain, and sub-cycle (down to 0.1 fs) localization, in the time domain. It is important that the density of hot spots, experiencing the special and temporal localization, in semicontinuous metal films is far larger than in fractal clusters.

The rest of the paper is organized as follows. In the next section we outline the idea standing behind the plasmon localization and describe the basic optical properties of semicontinuous metal films. In this section, we also show a close similarity between the problem of finding the EM field distribution over the film and the Anderson transition problem. In the same section, we describe the efficient method that allows us to find the EM field distribution over the film under excitation by monochromatic light. In Section 3, we present our method for finding the local temporal dynamics in the EM field distribution induced by a light pulse of *arbitrary* shape. In Section 4, we discuss results of our numerical simulations for the plasmon temporal dynamics induced by various laser pulses. Specifically, we consider there the excitation with rectangular and Gaussian laser pulses, and with a broadband, nearly continuous spectrum referred to as white light. The last Section concludes the paper.

2. PLASMON LOCALIZATION

Random metal–dielectric films can be prepared by deposition of metal onto a dielectric substrate. This can be done by laser ablation, thermal evaporation, or by other methods. In the growing process, first small metal particles are formed on the substrate. As the metal concentration grows, coalescence between the particles occurs and irregularly shaped metal clusters are formed. Finally, when the metal concentration p reaches the percolation threshold, p_c, a single conducting path from one side of the sample to another is formed so that the film becomes DC-conducting. Such film is referred to as semicontinuous metal film. Metal–dielectric films at different metal filling factors are shown in Fig. 1.

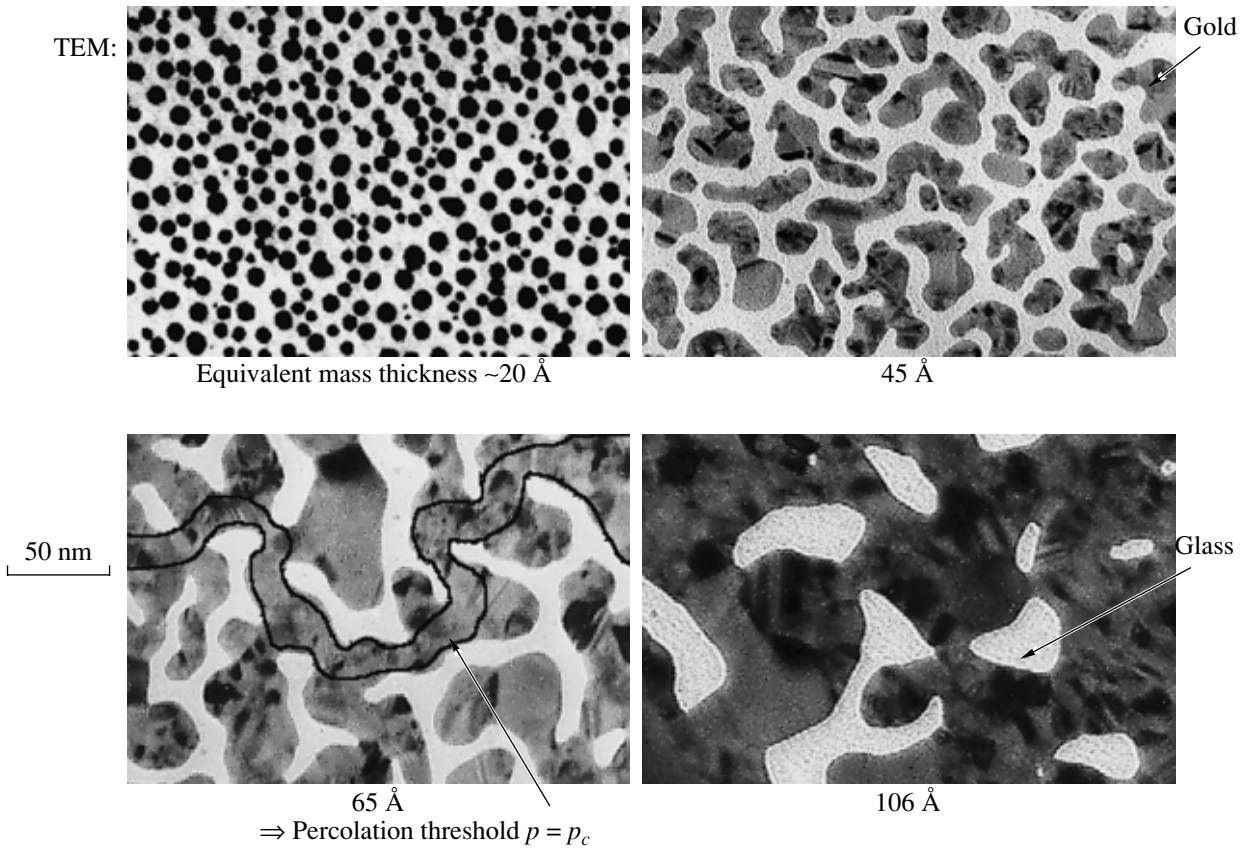

Fig. 1. TEM pictures of gold-glass films at different metal filling factors. Percolation (semicontinuous) film is formed at the effective gold-metal thickness 6.5 nm.

First, we consider the excitation of a semicontinuous metal film by a monochromatic wave at frequency ω. To find the EM field distribution over the sample, one must solve the equation describing the current conservation law

$$\nabla \cdot (\sigma(\mathbf{r})[-\nabla\phi(\mathbf{r}) + \mathbf{E}_e(\mathbf{r})]) = 0,$$

where $\phi(\mathbf{r})$ is the fluctuating local potential, $\sigma(\mathbf{r})$ is the local conductivity, and $\mathbf{E}_e$ is the excitation field. For simplicity, we assume that the applied EM field is directed along x axis. In the discretized form this equation acquires the form of the well-known Kirchhoff's equation

$$\sum_j \varepsilon_{ij}(\phi_i - \phi_j + E_{ij}) = 0,$$

where $\varepsilon = (4\pi i/\omega)\sigma$. If the period of the discretized lattice is a, then the discretized electromotive forces E_{ij} are taking values $E_e a$ for the bonds $\langle ij\rangle$ directed in $+x$ direction, $-E_e a$ for the bonds $\langle ij\rangle$ directed in $-x$ direction, and 0 for all other bonds. The dielectric constants ε_{ij} are equal to the dielectric permittivity of the dielectric, ε_d, and metal, ε_m, with the probabilities $(1-p)$ and p, respectively, where p is the metal filling factor. Below, we consider the case of a two-dimensional system at the percolation threshold $\left(p = p_c = \frac{1}{2}\right)$. In our approach, a percolation metal–dielectric film is modeled by a random network. The equation above can be rewritten in the matrix form, with the "interaction matrix" $\hat{H}$ (referred to as Kirchhoff's Hamiltonian, KH) defined in terms of the local dielectric constants:

$$\hat{H}\phi = E,$$

where ϕ is the N-dimensional vector of the local potentials, and E is the vector of local EM fields. The $N \times N$ matrix has off-diagonal elements $H_{ij} = -\varepsilon_{ij}$, and diagonal elements $H_{ii} = \sum_j \varepsilon_{ij}$ (j refers to the nearest neighbors of the site i). Matrix $\hat{H}$ is similar to the quantum-mechanical Hamiltonian for the Anderson transition problem with both on- and off-diagonal disorder [6, 7].

The dielectric constant of metal in the optical region can be well approximated by the Drude formula $\varepsilon_m(\omega) = \varepsilon_0 - (\omega_p/\omega)^2/[1 + i\omega_\tau/\omega]$, where ε_0 is the contribution to ε_m due to interband electron transition, ω_p is plasma frequency, and $\omega_\tau = 1/\tau$ is the relaxation rate. Typically, the dissipation in metal is relatively small in

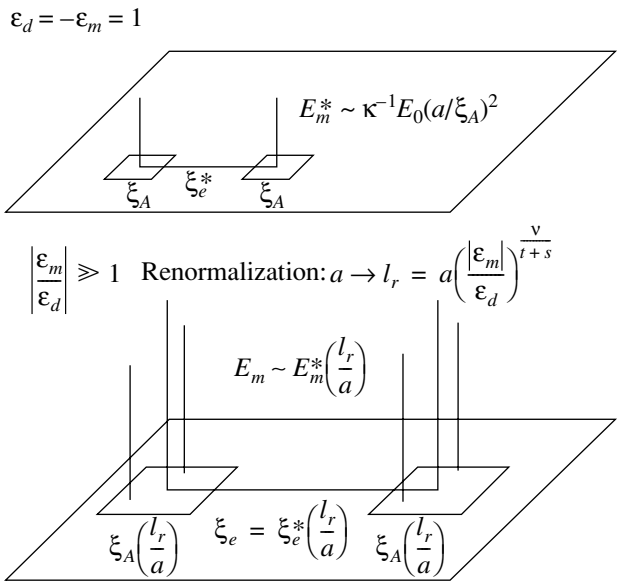

Fig. 2. Renormalization of the field distribution at the transition from the reference system with $-\varepsilon_m/\varepsilon_d = 1$ to the high-contrast system with $-\varepsilon_m/\varepsilon_d \gg 1$.

the high-frequency range, so that $\omega_\tau \ll \omega$. Therefore, the magnitude of the real part of ε_m ($|\varepsilon_m'|$) is much larger than the imaginary part, ε_m''. Accordingly, in the optical range, the "loss parameter" $\kappa = |\varepsilon_m''/\varepsilon_m'|$ is small. It is also important to note that the real part is negative for the frequencies lower then the "renormalized" plasma frequency $\tilde{\omega}_p = \omega_p/\sqrt{\varepsilon}$.

We first consider the special case of $\varepsilon_m = -\varepsilon_d$, with ε_d chosen, for simplicity, to be equal to one. In this case, all parameters of the KH are of the order of one, and the Hamiltonian is symmetric under the transformation $\varepsilon_m \longleftrightarrow \varepsilon_d$, so that the real eigenvalues are distributed symmetrically with respect to zero. The resonating eigenstates with eigenvalues close to zero are most effectively excited by the applied field. These eigenstates correspond to the localized in the space domain plasmon modes, which are known to result in giant field fluctuations on the surface of a percolation film [6, 7]. The maximum field enhancement in the "hot spots" is estimated as $E_m \sim E_0 \kappa^{-1} (a/\xi_a)^2$ [6, 7], where a is the size of particles, and ξ_A is so-called localization length, which is close in magnitude to a [6].

In the near-infrared and infrared parts of the spectrum, where $|\varepsilon_m'| \gg \varepsilon_d$ we use the following renormalization procedure (see Fig. 2). We divide our system into square regions of length l. Each square that has a conducting path from one side to the opposite is replaced by a single conducting element with effective dielectric constant $\varepsilon_m(l) = l^{-t/\nu}\varepsilon_m$, and each square that does not have a conducting path is replaced by a single dielectric element with the effective dielectric constant $\varepsilon_d(l) = l^{s/\nu}\varepsilon_d$, where the critical exponents are given by $t \simeq \nu \simeq s \simeq 4/3$ for $2D$ [1, 7]. Upon the renormalization, our system is changed to a new $2D$ percolation system; parameters of the new conducting and dielectric elements are chosen so that the optical properties of the original and renormalized systems were the same. As one can easily see, when the square size l is chosen as $l = l_r = a(|\varepsilon_m|/\varepsilon_d)^{\nu/(t+s)}$, the ratio of the dielectric constants is given by $\varepsilon_m(l_r)/\varepsilon_d(l_r) \cong \varepsilon_m/|\varepsilon_m| \approx -1 + i\kappa$, where the loss parameter $\kappa \approx \omega_\tau/\omega \ll 1$. Thus, after the renormalization, the problem becomes fully analogous to the case above, with $\varepsilon_d = -\varepsilon_m' = 1$. The field peaks, in this case, are estimated as $E_m \sim E_0(a/\xi_A)^2(|\varepsilon_m|/\varepsilon_d)^{\nu/(t+s)}(|\varepsilon_m|/\varepsilon_m'')$ [6, 7].

Because nonlinear processes involve local fields raised to the power greater than one, they are enhanced in percolation composites far stronger than the linear ones. The enhanced phenomena include, in particular, higher harmonic generation [8] and the white light generation (referred also to as super-continuum generation [9]. In the latter case, the white-light generation (WLG) from a semicontinuous metal film can be obtained at as low intensities as 10^9 W/cm^2, which is four to five orders of magnitude less than the intensities typically required for WLG in other media [7–9].

Thus, the field distribution in metal–dielectric percolation films, is extremely inhomogeneous, with the field intensity peaks localized in nm-sized areas and exceeding the applied field by 10^4 times. The phenomenon of localization of plasmons is a robust effect that occurs in a very broad spectral range from the near UV to the far IR. The actual spatial positions of "hot spots" are very sensitive to the wavelength and polarization of incident light. Figures 3a–3c show results of our numerical simulations of the field distribution for the same silver-glass percolation film at different wavelengths of the incident light. As the wavelength grows, the clusters of larger sizes begin to resonate; accordingly, the "hot spots" change their spatial positions so that the distance between them is growing with the wavelength [6]. The average magnitude of individual "hot spots" also grows with the wavelength before it saturates [6, 7]. Recent experiments of [3, 4, 7] have verified the plasmon localization as well as the described spectral dependence in the hot spot distribution (as an example, see Fig. 3d). The lower peak intensities in Fig. 3d as detected by scanning near-field optical microscope (SNOM), are explained by the fact that the apertureless SNOM used in the experiments employs a vibrating (in the z-direction) tip so that signals are averaged over a range of heights from 0 to 100 nm. The zero height corresponds to the maximum local-field enhancement ($I/I_0 \sim 10^4$ as shown in Figs. 3a–3c), whereas at the height of 100 nm the enhancement is practically absent [4].

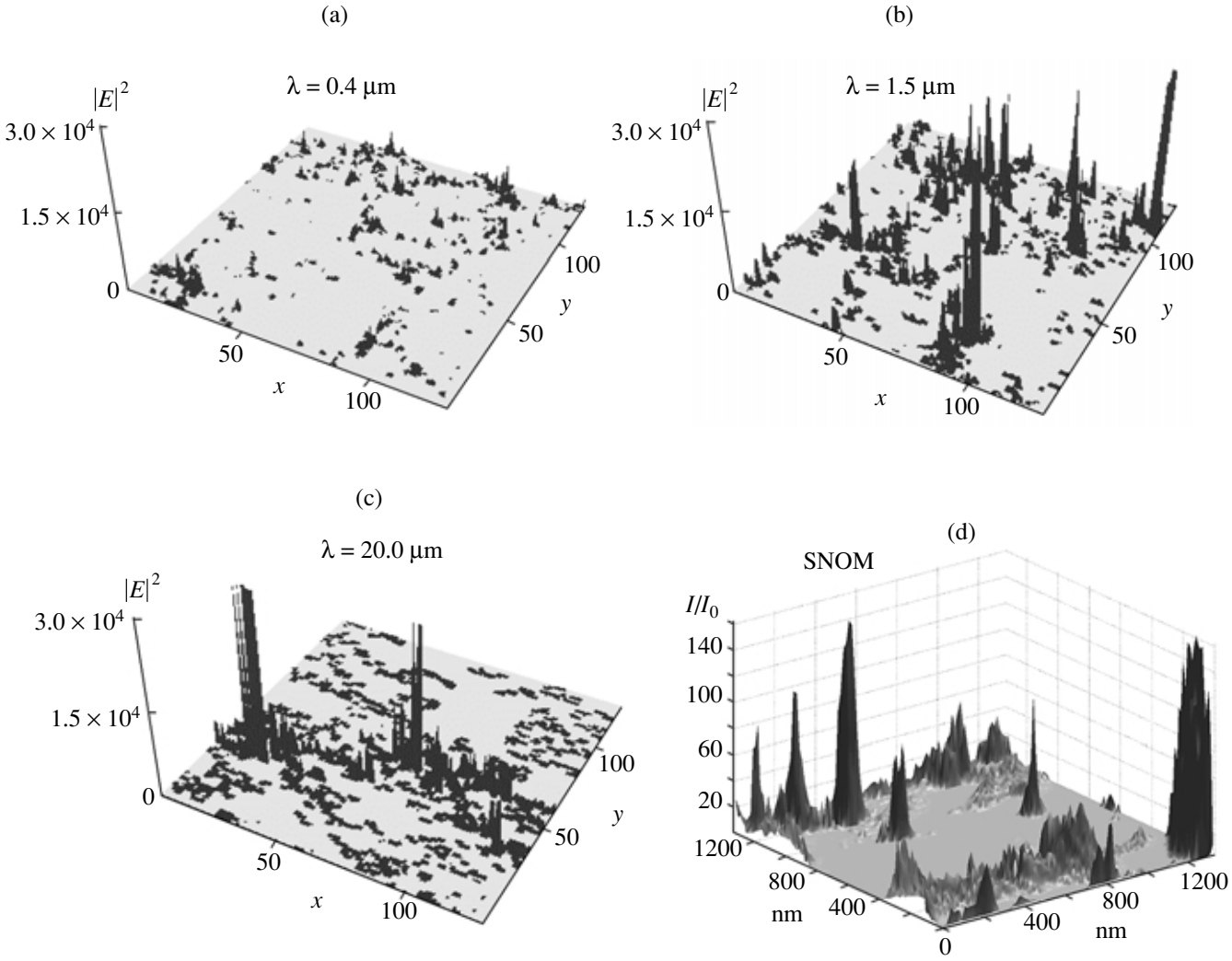

Fig. 3. Numerical simulations of EM field distribution over the same silver-glass percolation film (the film size is 1.2 μm) for different excitation wavelengths (a–c). (d) Shows the experimentally detected field distribution over the gold-glass percolation film, using scanning near-field optical microscope.

A metal–dielectric film at the percolation is scale-invariant so that clusters of all sizes, from individual particles up to the "infinite" percolation cluster spanning over the whole sample, are present and can be excited. As a result, such percolation film can support modes in a very broad spectral range, from the plasma frequency ω_p to the plasma relaxation rate ω_τ. The randomness of a percolation system also plays an important role, resulting in chaotic-like spatial distribution of "hot spots" and their spectral characteristics. Such statistically large system can *locally* have field fluctuations that are much shorter than the characteristic time for the average *macroscopic* response. As a result, the local field fluctuations can be significantly shorter than the pulse duration of the incident light, as opposed to the macroscopic optical response. To some extent, this is similar to the velocity distribution of molecules in gas, where individual velocities for some molecules can be greatly different from the thermal velocity. Thus, the localization and variety in local configurations of the resonating structures in a percolation film makes possible the excitation of modes from a very broad spectral range that, in turn, can result in extremely short local-field fluctuations.

3. METHOD

Methods available for finding the spatial field distribution in percolation films are well developed and described, for example, in [6, 7]. Here we use the approach that was suggested by Sarychev [6]. This method allows one to obtain the field distribution beyond the quasistatic approach, where the interaction of electric and magnetic fields with each other through the skin effect is taken into account.

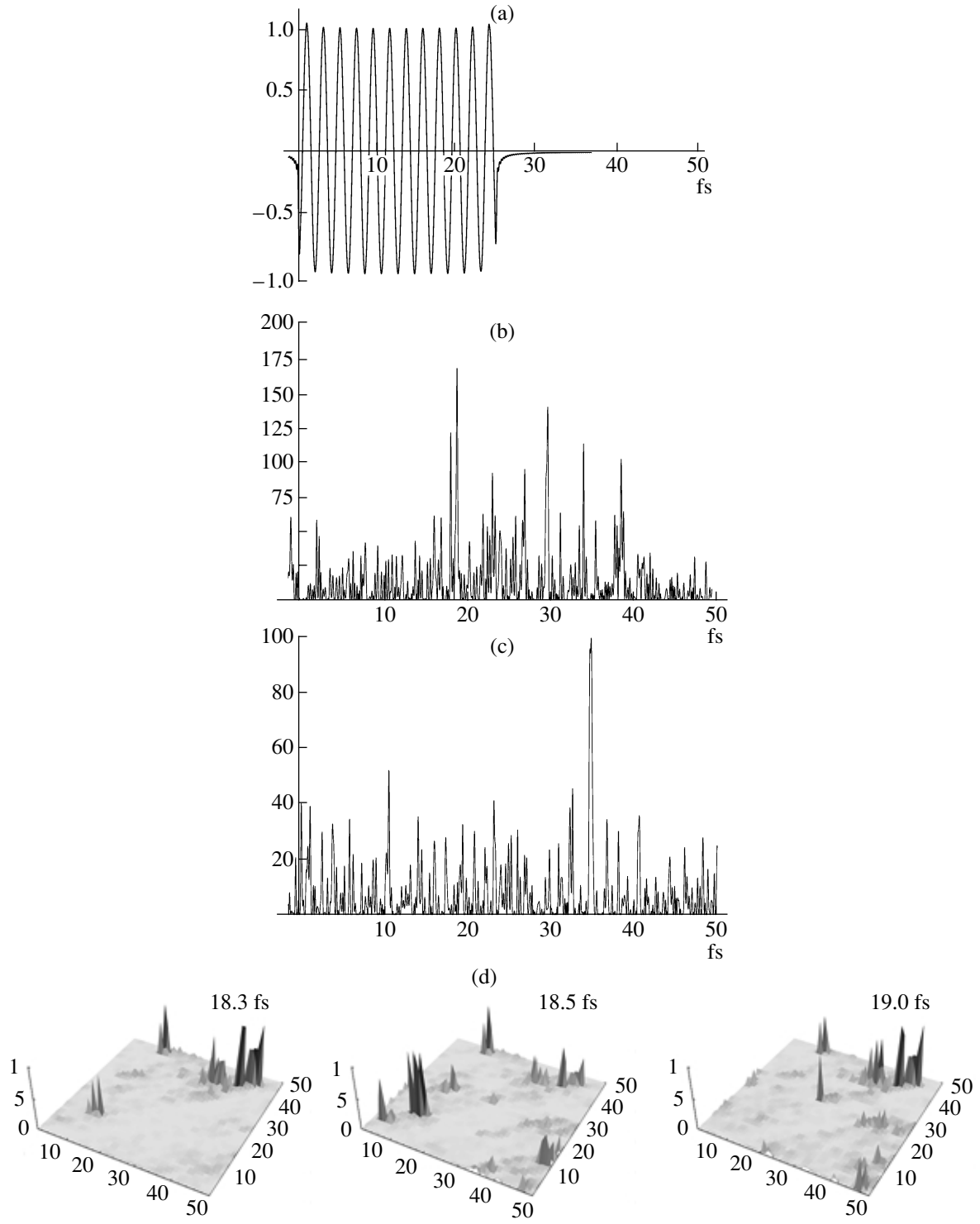

Fig. 4. Rectangular excitation pulse of 25 fs duration (a) and the local-field temporal dynamics induced by such excitation in two different points of the film [(b) and (c)]. (d) Shows the time-evolution of the field-intensity distribution over silver-glass percolation film. The excitation wavelength in all cases is 600 nm.

In the case of excitation by a monochromatic light the field distribution, $E(\mathbf{r})$, oscillates with the light frequency ω. Thus, the temporal dynamics of the system is given by $E(\mathbf{r})\exp(-i\omega t)$. In the case of excitation by arbitrarily shaped periodic wave $A(t)$, with the period T, the incident pulse can be represented by a Fourier series $A(t) = \sum_n A(\omega_n)\exp(-i\omega_n t)$, where $\omega_n = (2\pi n)/T$.

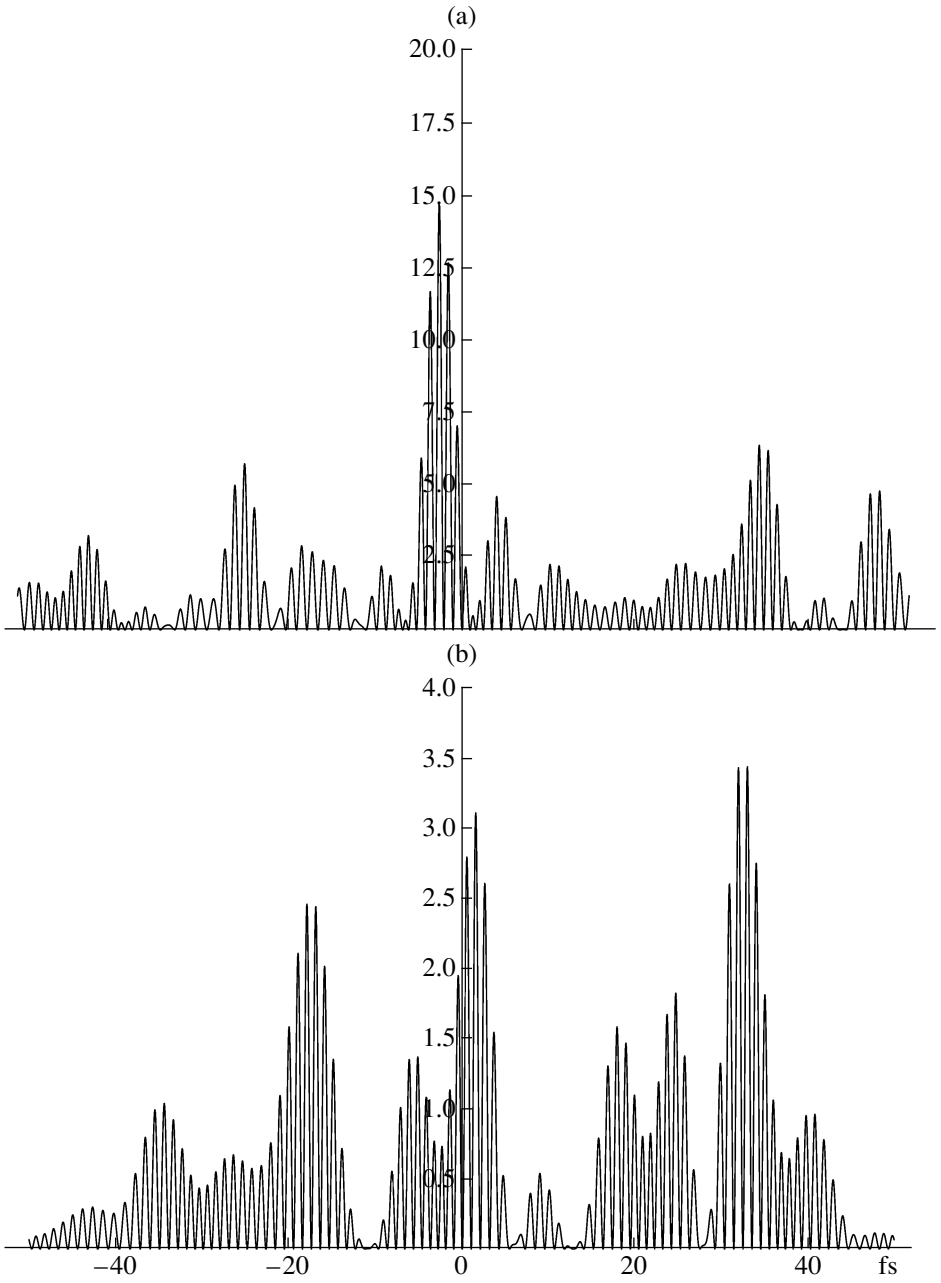

Fig. 5. Local field-intensity temporal dynamics for two spatially separated points at the excitation by Gaussian light pulse. The excitation pulse duration is 25 fs, wavelength is 600 nm.

Each Fourier harmonic is a monochromatic wave and the response to it, $E(\mathbf{r}, \omega_n)$, can be found by using the standard techniques mentioned above. Then, using the inverse Fourier transformation, we can obtain the local temporal response of the system for an arbitrarily shaped periodic laser pulse as $E(\mathbf{r}, t) = \sum_n E(\mathbf{r}, \omega_n) \exp(-i\omega_n t)$.

4. RESULTS

In our computer simulations we used three different shapes for the incident light pulses: Gaussian and rectangular pulses, and the white light. The pulse duration for the Gaussian and rectangular pulses were 25 fs, which is far below the plasmon life time, $\tau = 200$ fs. The carrying wavelength was 600 nm in all cases. As for the white light, we modeled it by a series of 400 harmonics (with random phases) from roughly 300 nm to 30 μm so that the intermode spacing was about 3×10^{12} Hz, which is significantly smaller than the plasma relaxation rate, $\omega_\tau = 5 \times 10^{12}$ Hz. Therefore, such a series of randomly phased harmonics can be considered as a nearly continuous spectrum that covers almost all the spectrum of a percolation film, from ω_p to ω_τ.

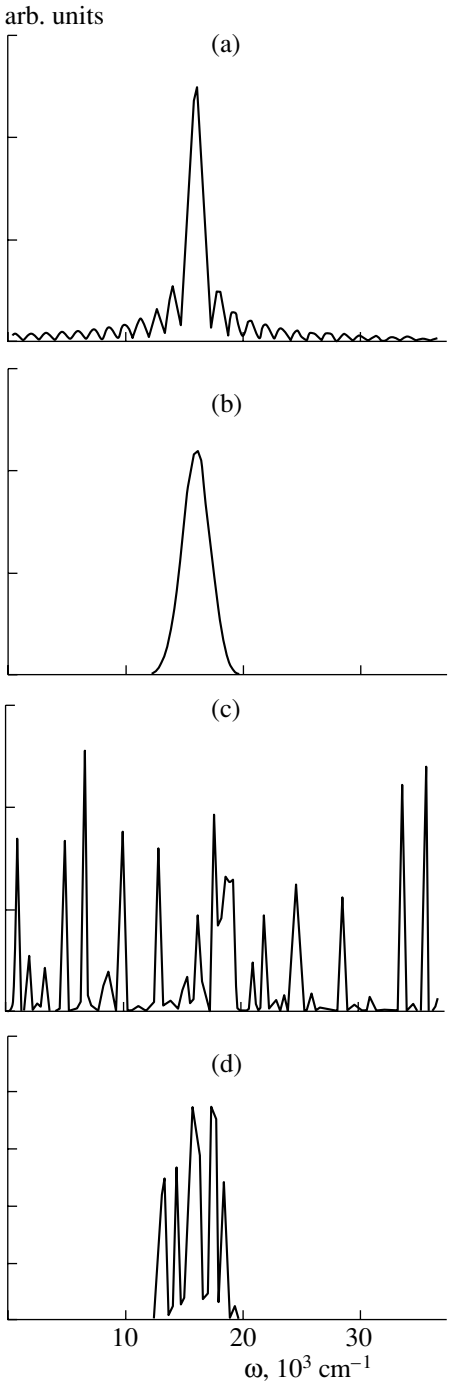

Fig. 6. Rectangular (a) and Gaussian (b) excitation 25-fs-pulse spectra and spectral distributions for the local response at some point of the film induced by 25-fs rectangular (c) and Gaussian (d) pulses.

When analyzing results of calculations, it is important to distinguish between sub-femtosecond dynamics and true sub-femtosecond pulses. Thus, the time response can experience a series of correlated "pulses," which are of nearly the same height and separated by time intervals comparable to (or even less than) the excitation light period; yet, the duration of a "cumulative pulse" can be much longer than the duration of a single "pulse." Accordingly, although one can speak, in this case, of a sub-fs dynamics there are no really sub-fs pulses. Such sub-fs dynamics occurs, for example, at the excitation by Gaussian light pulses in fractal clusters (see [5]) and in semicontinuous metal films, as considered below. As for real sub-fs pulses, they can be obtained at a broad-spectrum excitation, such as the one provided by a rectangular light pulse or by white light, as described below.

The temporal response of a percolation silver-glass film to a rectangular 25 fs pulse is shown in Fig. 4. The pulse itself is shown in Fig. 4a; Figs. 4b and 4c show the local-field intensity in two spatially-separated points of the film. Figure 4d shows time-evolution of the field distribution over the whole film within a sub-femtosecond time interval. Note the existence of local sub-fs pulses that can be probed using, for example, near-field optical microscopy/spectroscopy. It should be stressed that sub-fs pulses occur only *locally* in small, nm-sized areas of the system; they are averaged out when the macroscopic response is probed.

Indeed, it is hard to produce fs laser pulses that are close to rectangular shapes. Rather, laser pulses can typically be approximated by the Gaussian shape. We simulated the temporal response of a percolation film for the excitation by Gaussian 25 fs pulse. Local responses for two spatially separated points of a silver-glass percolation film are shown in Figs. 5a and 5b. As seen in Fig. 5, the local responses for the excitation by Gaussian pulses are longer than for the excitation by rectangular pulses. Still, it is important to note that the *local* responses can be several times shorter than the excitation pulse duration; again this effect can occur only locally and does not take place for the macroscopic response.

To explain the results above, we analyze the spectral characteristics of incident pulses and the local responses they induce. The spectra of the incident pulses, rectangular and Gaussian, are shown in Figs. 6a and 6b, respectively. In contrast to the Gaussian pulse, the rectangular pulse has long oscillating "wings" in its spectrum. In Figs. 6c and 6d, we show two spectra for the local response at the same spatial point induced by the excitation with rectangular and Gaussian pulses, respectively. As one can see, a broader spectrum of the rectangular excitation pulse results in a broader spectrum of the local response and, accordingly, in much shorter field fluctuations (cf. Figs. 4 and 5). These field fluctuations can be far shorter than the excitation pulse and even shorter than the light period. This occurs because the spectrally broader rectangular pulse can effectively excite far more plasmon modes than the Gaussian pulse. The constructive interference between these random modes can lead to the sub-fs fluctuations.

As mentioned, it is hard to produce rectangular pulses that could provide the broad-band excitation of

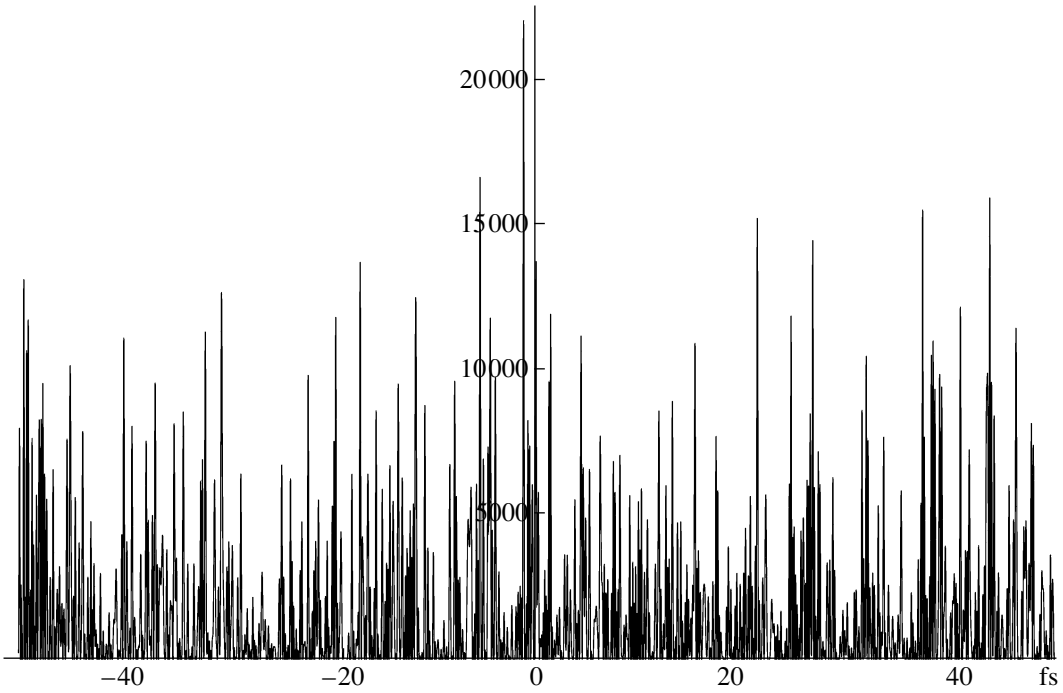

Fig. 7. Local field-intensity fluctuations at some point of a silver-glass percolation film under the white-light excitation.

a semicontinuous metal film needed for the generation of sub-fs pulses. In this sense, it looks more attractive to use the broadband white light that can be generated with conventional fs laser systems in many materials (including semicontinuous metal films themselves, where the WLG can be accomplished at rather moderate intensities [8, 9]). Because of the random nature of a percolation film one expects that "self-phasing" of plasmon modes at some points can occur, in this case, leading to sub-fs field fluctuations. Our simulation results shown in Fig. 7 vividly demonstrate the existence of such sub-fs field fluctuations on a silver-glass percolation film under excitation by the white light. Thus by using the broadband excitation source, such as the white light, one can locally generate sub-fs pulses that can be detected and utilized, for example, with the help of the near-field optical microscopy.

5. CONCLUSION

In conclusion, the scale-invariant morphology of percolation metal–dielectric films results in the spatial localization of plasmon modes, which because of a variety of the resonating structures, cover a very broad spectral range, from the near-UV to the mid-IR. By using a broadband excitation, one can induce the plasmon modes from a very broad spectral interval. This, in turn, can result in extremely short local-field fluctuations, far shorter than the pulse duration, and in some cases, shorter than the light cycle. Thus, semicontinuous metal films allow the sub-wavelength and sub-cycle localizations in the space and time domains simultaneously. Perhaps most attractive way to produce sub-fs pulses is to use the white light as a source of excitation of a semicontinuous metal film.

REFERENCES

1. Bergman, D.J. and Stroud, D., 1992, *Solid State Phys.*, **46**, 147.
2. Kreibig, U. and Vollmer, M., 1995, *Optical Properties of Metal Clusters* (Berlin: Springer).
3. Grésillon, S., Aigouy, L., Boccara, A.C., Rivoal, J.C., Quelin, X., Desmarest, C., Gadenne, P., Shubin, V.A., Sarychev, A.K., and Shalaev, V.M., 1999, *Phys. Rev. Lett.*, **82**, 4520.
4. Ducourtieux, S., Podolskiy, V.A., Grésillon, S., Berini, B., Gadenne, P., Boccara, A.C., Rivoal, J.C., Bragg, W.A., Banerjee, K., Safonov, V.P., Drachev, V.P., Ying, Z.C., Sarychev, A.K., and Shalaev, V.M., 2001, *Phys. Rev. B* (in press).
5. Stockman, M.I., 2000, *Phys. Rev. Lett.*, **84**, 1011; 2000, *Phys. Rev. B*, **62**, 10494.
6. Sarychev, A.K. and Shalaev, V.M., 2000, *Phys. Rep.*, **335**, 275.
7. Shalaev, V.M., 2000, *Nonlinear Optics of Random Media: Fractal Composites and Metal–Dielectric Films* (Berlin: Springer), STMP-158.
8. Breit, M., Podolskiy, V.A., Gresillon, S., von Plessen, G., Feldmann, J., Rivoal, J.C., Gadenne, P., Sarychev, A.K., and Shalaev, V.M., 2001, *Phys. Rev. B*, **64**.
9. Ducourtieux, S., Gresillon, S., Boccara, A.C., Rivoal, J.C., Quelin, X., Gadenne, P., Drachev, V.P., Bragg, W.D., Safonov, V.P., Podolskiy, V.A., Ying, Z.C., Armstrong, R.L., and Shalaev, V.M., 2000, *J. Nonlinear Opt. Phys. Mater.*, **9**, 105.